

PAPER • OPEN ACCESS

## Wave propagation in damage assessment of ground anchors

To cite this article: B Zima and M Rucka 2015 *J. Phys.: Conf. Ser.* **628** 012026

View the [article online](#) for updates and enhancements.

### You may also like

- [Combination of Edible Coating Green Grass Jelly and Cinnamon Essential Oil Increase the Shelf Life of Water Rose Apple Fruit](#)  
R R Apriliawati, S S Dewi and N A Utama
- [Investigation of plasma activated water in the growth of green microalgae \(\*Chlorella spp.\*\)](#)  
P Silapasert, C Yatongchai and S Sarapirom
- [Remote Sensing Dynamic Monitoring on the Land Destruction and Recovery of Green Mines](#)  
Weiling Yao, Jinzhong Yang, Na An et al.

**PRIME**  
PACIFIC RIM MEETING  
ON ELECTROCHEMICAL  
AND SOLID STATE SCIENCE

HONOLULU, HI  
Oct 6–11, 2024

Abstract submission deadline:  
**April 12, 2024**

Learn more and submit!

**Joint Meeting of**  
The Electrochemical Society  
•  
The Electrochemical Society of Japan  
•  
Korea Electrochemical Society

## Wave propagation in damage assessment of ground anchors

**B. Zima<sup>1</sup> and M. Rucka**

Department of Structural Mechanics, Faculty of Civil and Environmental Engineering, Gdańsk University of Technology, Poland

E-mail: [beazima@pg.gda.pl](mailto:beazima@pg.gda.pl)

**Abstract.** The inspection possibilities of ground anchors are limited to destructive test such as pull-out test. Guided wave propagation gives an opportunity to develop an inspection system dedicated to determine the condition of inspected element without violation of their integrity. In this paper the experimental study on wave propagation in laboratory models of ground anchors are presented. Experiments were conducted for different bonding lengths and different frequencies of excitation. Waves were generated by a piezoelectric actuator and the laser vibrometry technique was used to register velocity signals. For all tested anchors it was possible to identify the boundary between steel and concrete based on the registered reflections in wave propagation signals.

### 1. Introduction

The primary task of reinforced concrete elements, which are widely used in civil engineering is a significant load transfer achieved by the cooperation of concrete and reinforcing steel. Adhesion of concrete to steel is the most important component of load-bearing capacity of the element. The cooperation of steel and concrete in reinforced concrete structures is possible due to the binding, which consists of adhesion between steel and concrete, friction of steel on concrete clamping around due to shrinkage and mechanical resistances associated with the shaping surface of the bar and its configuration. The main problems of reinforced structures are slip or separation of two materials under load and in consequence, decrease of the load capacity. Moreover, it is an important issue because the visual assessment of the state is very often impossible after performing the item. Load capacity is determined during destructive testing which is based on applying gradually increasing load until destruction of tested structure. This method is very expensive, time consuming and requires performing elements, to be destroyed. Another drawback is the lack of information on other elements. Load capacity and workmanship of the group of elements is deduced on the base of investigation for one or few of them. For these reasons non-destructive diagnostic methods based on elastic waves propagation phenomenon have become the subject of intensive study over several last decades. In recent year, a large number of papers have been published on the use of guided waves for non-destructive evaluation (NDE) and structural health monitoring (SHM) and many of investigators have studied the guided wave propagation in various types of structures and materials, e.g. [1–10]. Wave propagation techniques offer the advantage of fast diagnostics of structural elements without violation of their integrity. They are totally adapted to automated inspection of large areas with a small number of sensors. That is the reason why methods based on wave propagation are very promising solutions for advanced monitoring systems or diagnostics of structures which cannot be assessed visually.

<sup>1</sup> To whom any correspondence should be addressed.



Very important group of relatively simply engineering structures made of a steel rod or tendon and concrete are ground anchors, which are used to support geotechnical structures. The tendon is a long element transferring only tensile force into deeper layers of the ground. The main element of the ground anchor is the anchor body. The compression of the soil causes resistance to movement of the whole element. Most common failures of the anchor systems are failures of the steel tendon caused by corrosion or failures of anchor body caused by weak condition of performed injected element [11]. Guided wave propagation gives an opportunity to assess the state of these elements without performing destructive tests called pull-out tests.

The study focuses on the identification and recognition of the phenomena, which occur during wave propagation in laboratory models of ground anchors with different bonding lengths. Different excitation frequencies have been tested with the aim to select the most sensitive frequency for detection of border of media and determination of the bonding length of the anchors.

## 2. Wave propagation phenomena in ground anchor

### 2.1. Wave modes in a free bolt

Waves propagating in a free rod are dispersive waves. The relationship between the frequency and the group velocity for guided waves propagating in a rod with a circular cross section can be obtained by solving the frequency equation known as the Pochhammer equation [12]. The equation has the following form [13]:

$$\frac{2\alpha}{r}(\beta^2 + k^2)J_1(\alpha r)J_1(\beta r) - (\beta^2 - k^2)^2 J_0(\alpha r)J_1(\beta r) - 4k^2\alpha\beta J_1(\alpha r)J_0(\beta r) = 0, \quad (1)$$

where:

$$\alpha^2 = \frac{\omega^2}{c_L^2} - k^2, \quad (2)$$

$$\beta^2 = \frac{\omega^2}{c_s^2} - k^2, \quad (3)$$

$$k = \frac{\omega}{c}, \quad (4)$$

and  $r$  denotes a radius of the rod,  $k$  is the wavenumber,  $\omega$  is a circular frequency.  $J_0$  and  $J_1$  are the Bessel functions of the first kind. Velocities of the bulk waves, i.e. the velocity of the pressure wave  $c_L$  and the velocity of the shear wave  $c_s$  are defined as:

$$c_L = \left( \frac{E(1-\nu)}{\rho(1+\nu)(1-2\nu)} \right)^{1/2}, \quad (5)$$

$$c_s = \left( \frac{E}{2\rho(1+\nu)} \right)^{1/2}, \quad (6)$$

where  $\rho$  denotes the density,  $E$  is the Young modulus and  $\nu$  is the Poisson coefficient.

### 2.2. Wave propagation on the border of the media

At the interface between media with different physical properties two phenomena may occur: the wave can be reflected from the boundary or it can be transmitted into the second medium (Figure 1). The intensity of the reflection and the transmission depends on the difference between values of the acoustic impedance of two media. In the case of two media with different values of longitudinal wave



velocity, only the part of the wave energy penetrates into the second medium, while the remaining part is reflected. A large difference in the impedance can result in complete reflection of wave, while a small difference in the impedance may be the cause of the dominance of the wave transmission into the surrounding medium.

The intensity of the leakage of the wave energy not only depends on material parameters of two media but also on the bonding length and the quality of connection. The difference in the quality of the connection between steel and concrete can be noticed when the intensity of the leakage for two different cases (destroyed and undestroyed anchor) is compared. When the bonding quality is high, the transfer of the energy to the surrounding medium is more effective and results in greater leakage of the energy. When the bonding is weak, the phenomenon of wave reflection from the border of media dominates (Figure 2).

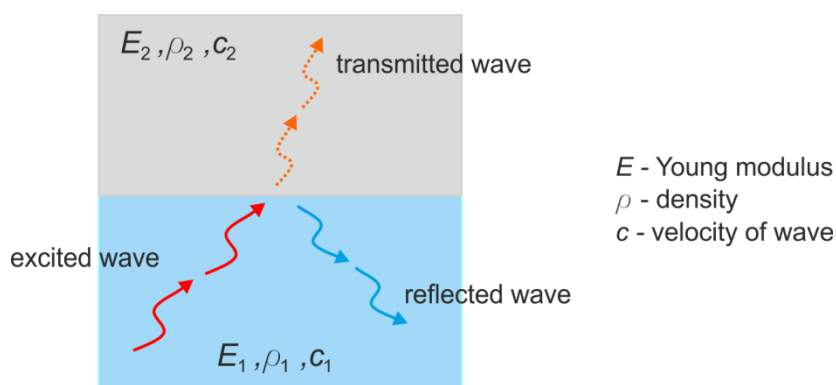


**Figure 1.** Wave reflecting and passing through the boundary between media

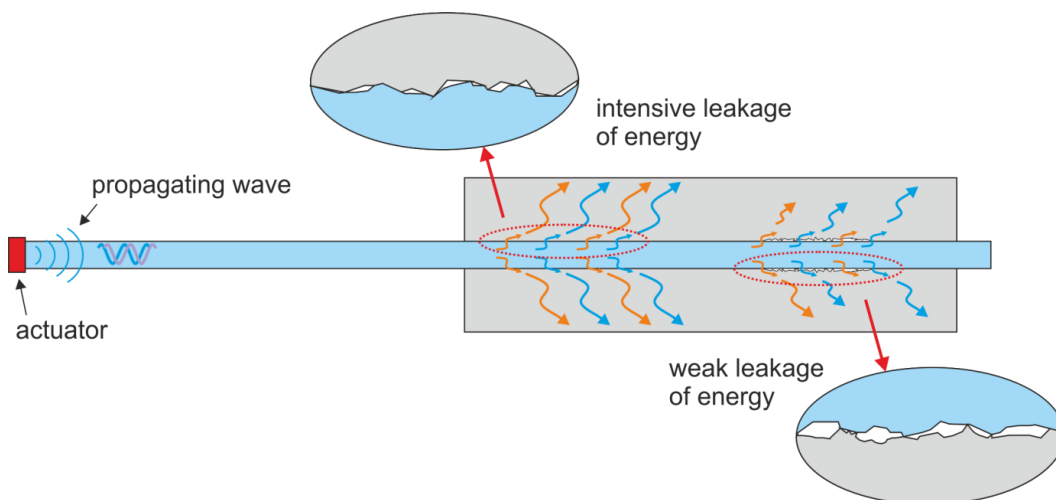


**Figure 2.** Wave leakage on the steel-concrete interface

### 3. Experimental investigation

#### 3.1. Ground anchor specimens

Laboratory models of ground anchors were considered as testing structures. The ground anchor consists of a steel circular rod having diameter of 2 cm and 150 cm long embedded in concrete cylinder having outer diameter of 10 cm and the length  $a$ . The geometry of the model is presented in Figure 3. Nine different cases of bonding length were considered, namely  $a = 0, 10, 20, 30, 40, 50, 60, 80, 100$  cm. The material parameters were for steel:  $E = 210$  GPa;  $\nu = 0,3$ ;  $\rho = 7820$  kg/m<sup>3</sup> and for concrete:  $E = 26$  GPa;  $\nu = 0,2$ ;  $\rho = 2084$  kg/m<sup>3</sup>.



### 3.2. Experimental set-up

Experimental set-up is shown in Figure 4. Guided waves were excited by the arbitrary waveform generator (Tektronix AFG 3022) with the high voltage amplifier (EC Electronics PPA 2000). The PZT actuator was bonded on the left end of the steel rod. By the use scanning head of the laser vibrometer Polytec PSV-3D-400-M propagating velocity signals  $v(t)$  were sensed and recorded parallel to the rod axis on the same end where the excitation was realized.

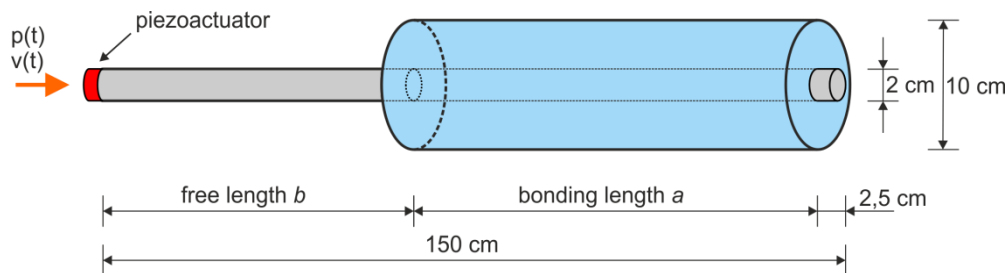


**Figure 3.** Geometry of the tested specimen



**Figure 4.** Experimental set-up for wave propagation measurements of ground anchors

As the excitation signal a wave packet was used (Figure 5). It was obtained by multiplying a 5-cycle sinusoidal function of carrier frequency  $f$  and a window function  $w(t)$ :

$$p(t) = \begin{cases} p_o \sin(2\pi ft) \cdot w(t) & t \in [0, T_w], \\ 0 & t > T_w, \end{cases} \quad (7)$$

where  $T_w$  is the length of a window and  $p_o$  denotes an amplitude of a sinusoidal function. As a window function, the Hanning window was chosen:

$$w(t) = 0.5(1 - \cos(2\pi ft / n_w)), \quad t \in [0, T_w], \quad (8)$$

where  $n_w$  is the number of counts in the tone burst. The carrier frequency  $f$  of the wave packet varied from 30 kHz to 90 kHz with the step of 10 kHz.

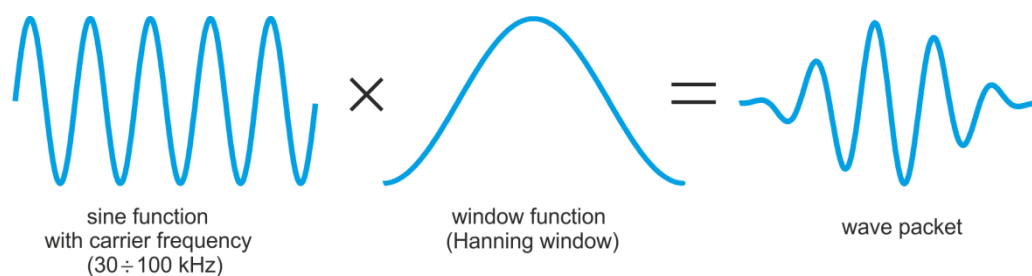


**Figure 5.** Wave excitation signal used in experimental investigations

### 3.3. Dispersion curves for a free rod

The solution of the Pochhammer equation can be presented graphically as dispersion curves. The lowest longitudinal mode  $L(0,1)$  is the most important from the practical point of view in the context of non-destructive diagnostics. In Figure 6 numerical and experimental results are compared. Numerical curves were calculated based on Eq. (1) in the frequency range up to 300 kHz. In this range, besides the fundamental mode, two higher longitudinal modes appear above their cut-off frequencies:  $L(0,2)$  and  $L(0,3)$  modes. Experimental part of the curve was determined by dividing the distance equal to twice the length of the rod by the time interval between registration peaks of incident and reflected wave packet.

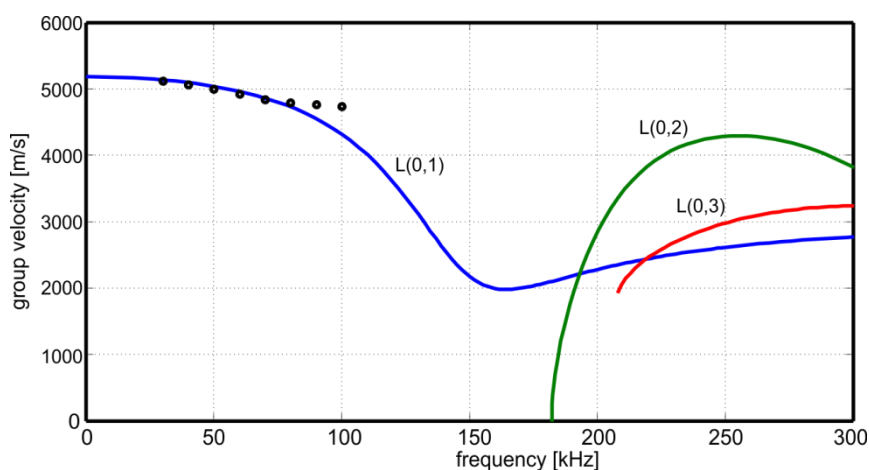


**Figure 6.** Group velocity dispersion curves: (—) numerical results (solutions of Pochhammer equation); (o) experimental results

## 4. Results of experimental investigations

### 4.1. Selection of excitation frequency

Before the assessment of condition of ground anchors, the selection of appropriate frequency of excitation was performed. At first, experimental investigation was performed for the free rod in the frequency range 30–100 kHz. Figure 7 shows envelopes of wave propagation signals created using the Hilbert transform. The envelopes of the vibration velocity signals were normalized with respect to the input wave amplitude by the following formula:

$$\hat{v}_n(t) = \frac{\hat{v}(t)}{\max(\hat{v}(t))}, \quad (9)$$

where  $\hat{v}(t)$  is the spectrum of the Hilbert transform of velocity signal  $v(t)$ . In the time interval from 0 ms to 1.5 ms the incident wave and two reflections are visible. It can be observed that the amplitude of the first and second reflections from the end of the rod varies with the change of frequency of

incident wave. Even though reflections for all considered frequencies are clear, a significant difference between amplitude values for different carrier frequencies can be observed. With the increase of the excitation frequency, the increase of the first and second reflection can be observed. The maximum value was archived for the frequency of 90 kHz (Figure 7).

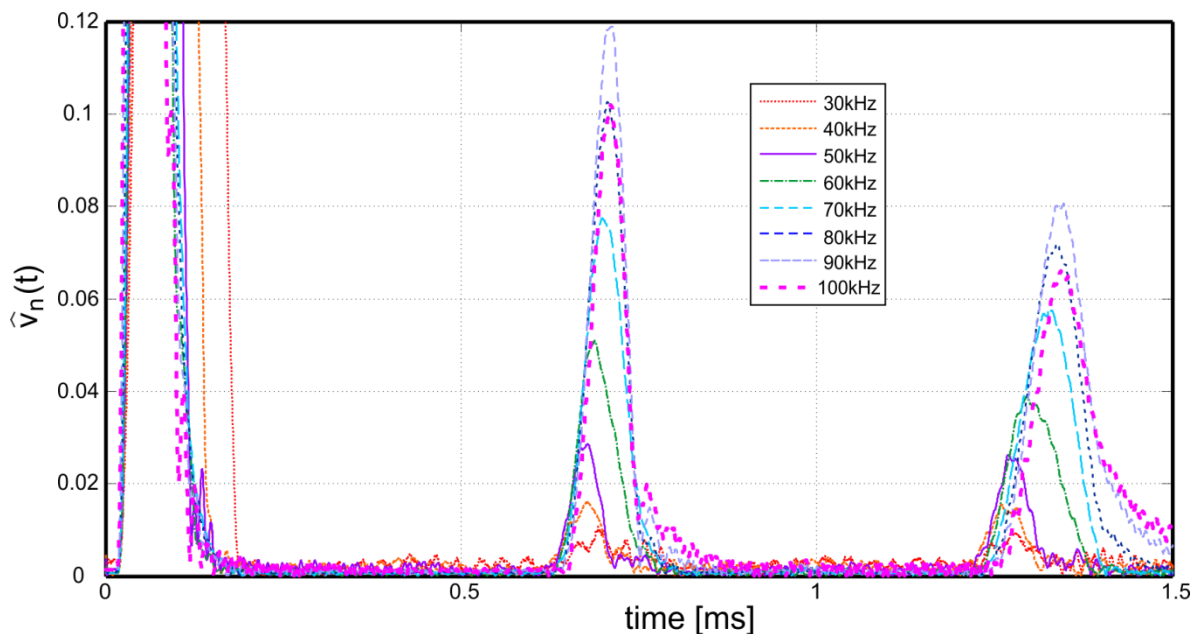


**Figure 7.** Set of wave propagation signals (in the form of signal envelopes) collected during experiments for different carrier frequency of excitation for the free rod

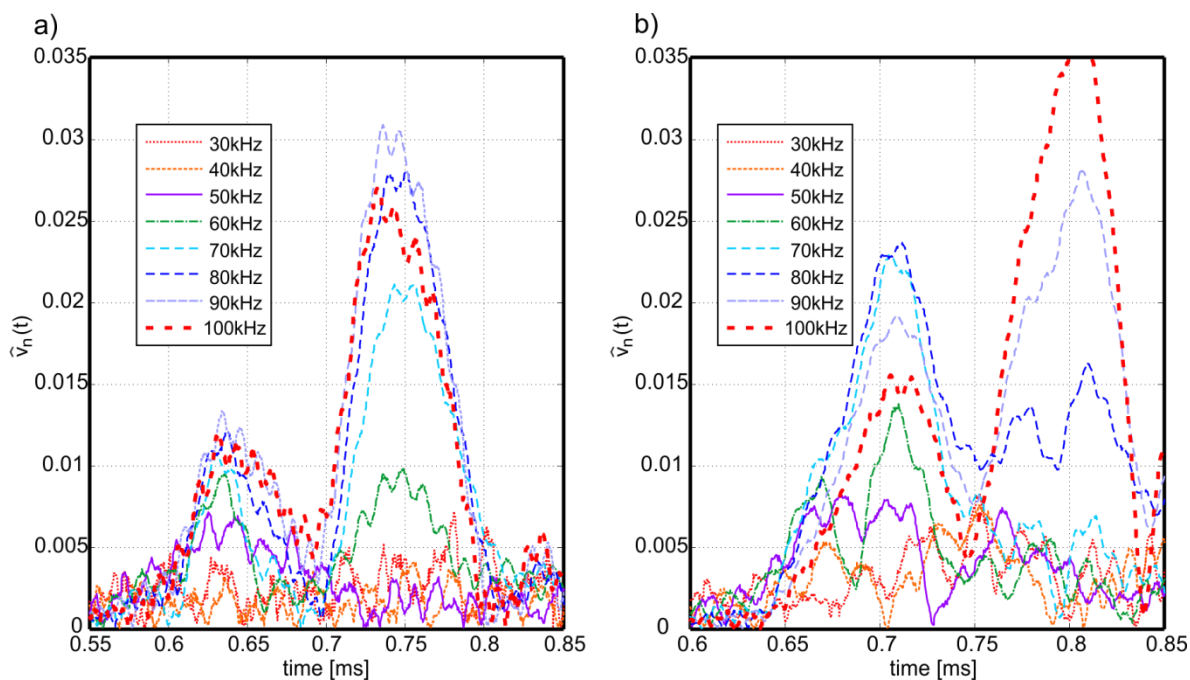


**Figure 8.** Set of reflections from anchorage collected during experiments for different carrier frequency of excitation for anchor with bonding length equal to: a) 20 cm, b) 40 cm

The increase of the amplitude proportional to the increase of the excitation frequency has been also observed for the rest of the anchors. An example of results for two different bonding lengths ( $a = 20$  cm and  $a = 40$  cm) are shown in Figure 8. This comparison allowed establishing that further analysis should include the propagation of waves with a carrier frequency equal to 90 kHz, because the energy of reflection was the highest for this frequency.

#### 4.2. Identification of bonding lengths

In Figure 9, a set of wave propagation signals for all tested bonding lengths and for chosen carrier frequency equal to 90 kHz are presented. Due to the leakage of the energy caused by surrounding concrete, the reflections from the end of the steel rod are not visible. The wave packets highlighted in Figure 9 result from the wave reflection from the anchorage, i.e. the boundary between steel and concrete. One can see that the length of the propagation path is proportional to the time interval between the registered incident wave and the reflected wave. In consequence this time interval is in inverse proportion to the bonding length.

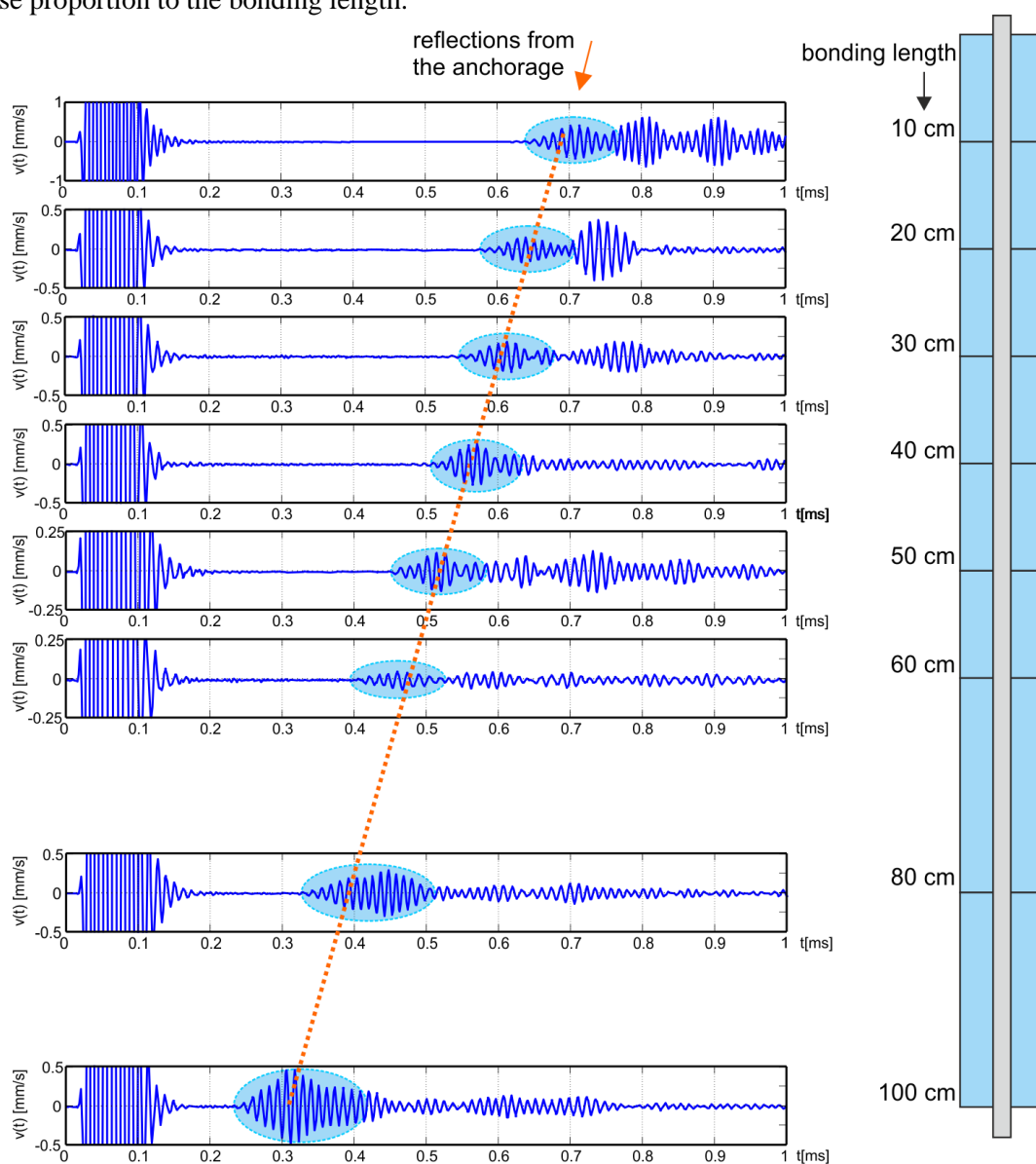


**Figure 9.** Set of signals collected during experiments for carrier frequency of excitation equal to 90 kHz and for different bonding lengths with indicated reflections from the anchorage



## 5. Conclusions

This paper presents an experimental investigation of guided wave propagation in laboratory models of ground anchors. The specimens with different bonding lengths were tested by the wave packet excitation with different carrier frequencies. The main conclusions are connected with the fact that properties of guided waves, such as attenuation or velocity, are functions of the input wave frequency. As the bonding length increases and the quality of the connection between steel rod and concrete gets better, the more energy of wave is transferred into concrete and the amplitude quickly attenuates. In investigated anchors, even for relatively short bonding lengths, the dissipation of energy was enough intensive to prevent extraction of information about reflection from the end of the rod. For all tested anchors it was possible to identify the boundary between steel and concrete based on reflections in the registered wave propagation signals.

## 6. References

- [1] Park H. W., Sohn H., Law K. H., Farrar C. R. Time reversal active sensing for health monitoring of a composite plate. *Journal of Sound and Vibration*, vol. 302, 2007, pp. 1907–1914.
- [2] Yu L., Giurgiutiu V. In situ 2D piezoelectric wafer active sensors arrays for guided wave damage detection. *Ultrasonics*, vol. 48, 2008, pp. 117–134.
- [3] Mallet L., Lee B., Staszewski W. J., Scarpa F. Structural health monitoring using scanning laser vibrometry: II: Lamb waves for damage detection. *Smart Materials and Structures*, vol. 13, 2004, pp. 261–269.
- [4] Żak A., Radziński M., Krawczuk M., Ostachowicz W. Damage detection strategies based on propagation of guided elastic waves. *Smart Materials and Structures*, vol. 21, 2012, 035024.
- [5] Malinowski P., Wandowski T., Ostachowicz W. Damage detection potential of a triangular piezoelectric configuration. *Mechanical Systems and Signal Processing*, vol. 25(7), 2011, pp. 2722–2732.
- [6] Rucka M. Experimental and numerical study on damage detection in an L-joint using guided wave propagation. *Journal of Sound and Vibration*, vol. 329, 2010, pp. 1760–1779.
- [7] Rucka M., Wilde K. Experimental study on ultrasonic monitoring of splitting failure in reinforced concrete. *Journal of Nondestructive Evaluation*, vol. 32, 2013, pp. 372–383.
- [8] Alleyne D. N., Pavlakovic B., Lowe M. J. S., Cawley P. Rapid, long range inspection of chemical plant pipework using guided waves. *Key Engineering Materials*, 270–273, 2004, pp. 434–441.
- [9] Ciang C. C., Lee J. R., Bang H. J. Structural health monitoring for a wind turbine system: a review of damage detection methods *Measurements science and Technology* vol. 19(12), 2008, 122001.
- [10] Beard M. D., Lowe M. J. S. 2003 Non-destructive testing of rock bolts using guided ultrasonic waves *International Journal of Rock Mechanics and Mining Sciences* vol. 40, 2003, pp. 527–536.
- [11] Sabatini P.J., Pass D.G., Bachus R.C. Ground anchors and anchored systems – Technical Report FHWA-IF-99-015, Office of Bridge Technology, Washington, 1999.
- [12] Pochhammer L. Beitrag zur Theorie der Biegung des Kreiscylinders. *Journal für die reine und angewandte Mathematik* 81, 1876, pp. 33–61.
- [13] Achenbach J.D. *Wave propagation in solids*. North-Holland Publishing Company, 1975.